ACS APPLIED MATERIALS & INTERFACES

Research Article

www.acsami.org

pH-Controllable Water Permeation through a Nanostructured Copper Mesh Film

Zhongjun Cheng,[‡] Ming Du,[‡] Kewei Fu,[‡] Naiqing Zhang,[†,‡] and Kening Sun*[,†,‡]

[†]State Key Laboratory of Urban Water Resource and Environment, School of Municipal and Environmental Engineering, and [‡]Natural Science Research Center, Academy of Fundamental and Interdisciplinary Sciences, Harbin Institute of Technology, Harbin, Heilongjiang 150090, P. R. China

Supporting Information

ABSTRACT: Water permeation is an important issue in both fundamental research and industrial applications. In this work, we report a novel strategy to realize the controllable water permeation on the mixed thiol (containing both alkyl and carboxylic acid groups) modified nanostructured copper mesh films. For acidic and neutral water, the film is superhydrophobic, and the water cannot permeate the film because of the large negative capillary effect resulting from the nanostructures. For basic water, the film shows superhydrophilic property, and thus the water can permeate the film easily. The permeation process of water can be controlled just by simply altering the water pH. A detailed investigation indicates that nanostructures on the substrate and the appropriate size of the microscale mesh pores can enhance not only the static wettability but also the dynamic properties. The excellent controllability of water permeation is ascribed to the combined effect of the chemical variation of the carboxylic acid group and the microstructures on the substrate. This work may provide interesting insight into the new applications that are relevant to the surface wettability, such as filtration, microfluidic device, and some separation systems.

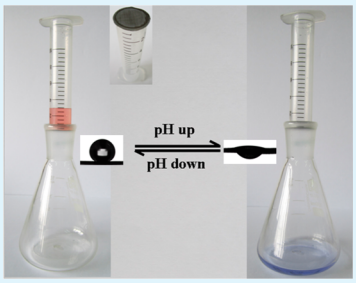

KEYWORDS: *pH-responsive, water permeation, superhydrophobic, superhydrophilic, nanostructure*

INTRODUCTION

Since the water permeation process is crucial and ubiquitous in industry, agriculture, and living systems,[1−6] there is an increasing need to realize controllable water permeation because of its significant implications for the understanding of biological activities and the design of novel microfluidic devices. In the past few years, many novel materials[7,8] and new technologies[9,10] have been advanced for controllable permeation, such as zeolite membranes,[7] carbon nanotube film,[8] and other smart copolymers.[11,12] However, all have proved to be rather cumbersome or need costly precursors.

Recently, a novel surface with switchable wettability has aroused research interest because of the ability for reversible transition between the superhydrophobicity and superhydrophilicity.[13−15] On such a surface, the water droplet usually takes a quasi-spherical shape with a contact angle larger than 150° when the surface is superhydrophobic, and it spreads quickly as the surface becomes superhydrophilic with a contact angle lower than 10°. The transition can be controlled by the external stimulus. Until now, many materials with such ability have been prepared by the combination of responsive molecules and rough microstructures,[16−38] for example: temperature-responsive poly(*N*-isopropylacrylamide) modified silicon pillars,[16] light-induced arrays of ZnO nanorods[17] and lotus-like TiO_2 film,[18] electrochemical triggered polypyrrole surface,[19] and some others that are responsive to solvent[20] and pH.[21,22] It can be noted that all the research is focused on the enhanced effect of the nanostructures on the static transition of wettability on the solid surface. Nevertheless, research regarding the dynamic properties enhanced by the nanostructures and the transition on the porous materials such as reticulated film is also important, since it is expected that such a study would provide facile methods or new materials for the controllable water permeation. Until now, correlative reports are still rare.[39−43]

Herein, based on the above concept, we report a novel strategy to realize the controllable water permeation on the nanostructured copper mesh film, which can transit between a superhydrophobicity and superhydrophilicity responsive to water pH. Such smart films were fabricated by assembling the mixed thiol (containing both an alkyl and carboxylic acid group) on the nanostructured copper mesh substrate. For acidic and neutral water droplets, the film shows superhydrophobic property, and thus water cannot permeate the film for large negative capillary effects resulting from the nanostructures. For basic water, the film is superhydrophilic, and thus the water can permeate the film easily. The permeation of water through the mesh film can be controlled by simply changing the pH of water. Furthermore, it can be found that the nanostructures on the substrate and the appropriate size of the microscale mesh pores can enhance not only the static wettability but also the dynamic properties, which is crucial in the excellent controllability of water

Received: July 26, 2012
Accepted: October 22, 2012
Published: October 22, 2012

   dx.doi.org/10.1021/am3014746 | ACS Appl. Mater. Interfaces 2012, 4, 5826−5832

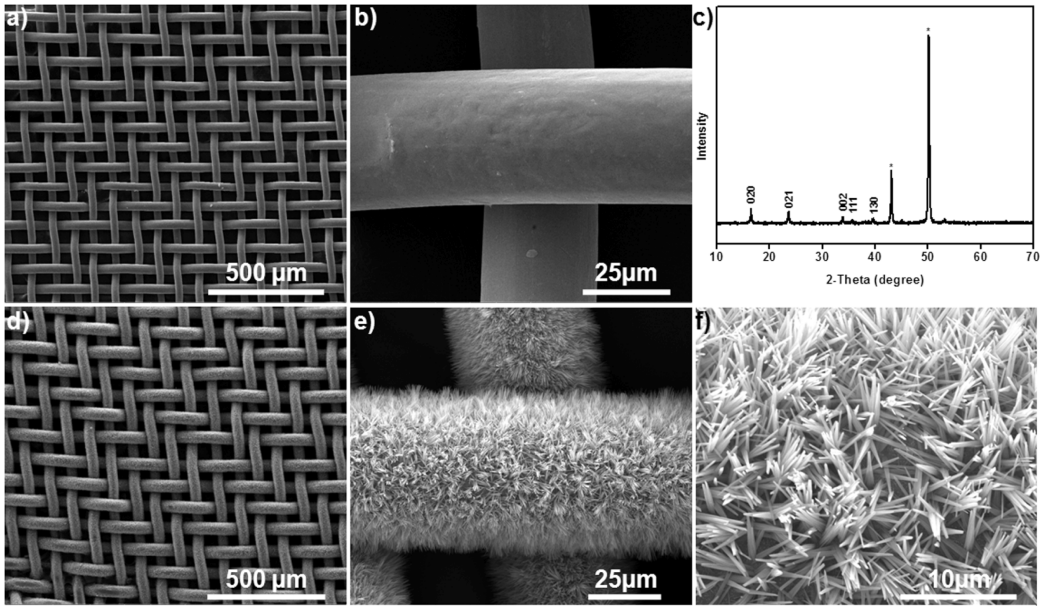

Figure 1. (a, b) SEM images of original copper mesh with low and high magnification, respectively. (c) XRD pattern of the substrate after anodization, indicating that $Cu(OH)_2$ was produced. (d–f) SEM images of rough copper mesh substrate with different magnifications.

permeation on the film. This work may be promising for new applications of materials with changing wettability in controllable filtration, microreactors, and microfluidic devices.

EXPERIMENTAL SECTION

Materials. Copper mesh foils (99.9%) were purchased from Shanghai Chemical Reagent Co., China. The copper mesh is composed of a single layer of copper wires with square pores, and the thickness is approximate with the diameter of the copper wire. The diameters of the copper wires for all mesh substrates are fixed (about 35 μm), and the size of the mesh pores changes from 35 to 160 μm. A stainless steel sheet (AISI 304), KOH (≥84%; Beijing Fine Chemical Co., China), $HS(CH_2)_9CH_3$, $HS(CH_2)_{10}COOH$ (Aldrich, Germany), and ethanol were used as received. Double-distilled water (>1.82 MΩ cm, Milli-Q system) was used.

Fabrication of the Nanostructured $Cu(OH)_2$ on the Copper Mesh Substrates. The anodization of a copper mesh substrate in an aqueous solution of KOH was used to produce the $Cu(OH)_2$ nanostructures on the substrate. The growth of $Cu(OH)_2$ nanoneedles was carried out at room temperature in a one-compartment cell controlled on an electrochemical workstation (CHI 660D, Shanghai Huachen Instrument Co., China). The copper mesh foil (surface area = 7.5 cm^2) was used as the working electrode, and the stainless steel sheet (surface area = 8 cm^2) was used as the counter electrode. The solution was deaerated by a dry nitrogen stream and maintained at a light overpressure during the experiments. The $Cu(OH)_2$ film was electrochemically grown at a constant current density of 1.5 mA cm^{-2} in KOH aqueous solution (2 mol L^{-1}) at different time. After reaction, the copper mesh substrate with $Cu(OH)_2$ was taken out from the solution and washed with distilled water and dried with N_2 stream.

Assembly of Responsive Molecules on the Copper Mesh Substrates. After fabrication of the $Cu(OH)_2$, the copper mesh substrates were first coated with a layer of Au (using a sputter-coater K575XD, Quorum) and then immersed into the mixed thiol solution of $HS(CH_2)_9CH_3$ and $HS(CH_2)_{10}COOH$ for approximately 12 h. The mole fraction of the mixed solution of $HS(CH_2)_{10}COOH$ and $HS(CH_2)_9CH_3$ was varied while keeping the total concentration of the thiol in solutions constant at 1 mmol L^{-1} in the ethanol solution. Finally, the substrate was taken out of the solution and washed with ethanol and dried with N_2 stream. The flat copper surfaces were fabricated by simply immersing the clean flat copper substrates into the mixed thiol with X_{COOH} = 0.6 (mole fraction of $HS(CH_2)_{10}COOH$ in the modified solution) for about 12 h and then washed with ethanol and dried with N_2 stream.

Instrumentation and Characterization. A field-emission scanning electron microscope (FEI, Quanta 200f) was used to obtain SEM images of the substrates, and static, advancing, and receding contact angles were measured on a JC 2000D5 (Shanghai Zhongchen Digital Technology Apparatus Co., Ltd.). The average contact angles were obtained by measuring at five different points with constant water droplet volume (4 μL) on the same film. For acidic and neutral water droplets, the static photographs of the water droplet on the films are just needed, and for a basic water droplet, it can spread and permeate through the film; a CCD camera was used to capture the process. X-ray diffraction spectroscopy data were carried out by using an X-ray diffractometer model D8 advance (Bruker) with Cu Kα radiation (λ = 1.5418 Å). X-ray photoelectron spectroscopy data were obtained with a K-Alpha electron spectrometer (Thermofisher Scientific Co., USA) using Al Kα (1486.6 eV) radiation. The base pressure was about 1×10^{-8} mbar. The binding energies were referenced to the C1s line at 284.8 eV from adventitious carbon. The photos in Figure 4 were obtained by a camera (FINEOIX F85 EXR). The acidic droplet was the aqueous solution containing the hydrochloric acid, and the basic droplet was the aqueous solution containing the sodium hydroxide. The pH value of the solution was measured by the pH meter (PB-10 Sartorius).

RESULTS AND DISCUSSION

To realize the controllable water permeation, a substrate with proper porous structure often is necessary.[40,41] In this work, copper mesh substrates were chosen for their wide applications in industrial production. Figure 1a shows the typical scanning electron microscopy (SEM) image of the original smooth copper mesh substrate. The diameter of one copper wire and the size of one square pore is about 35 and 58 μm, respectively (Figure 1b). After the anodization in an aqueous solution of KOH, a layer of nanostructured $Cu(OH)_2$ can be produced on the copper mesh substrate (for more details see Supporting Information Figures S1 and S2). As shown in the X-ray diffraction (XRD) patterns (Figure 1c), all the indexed diffraction peaks except those marked with stars (attributed to the copper substrate) can be indexed to the orthorhombic phase of $Cu(OH)_2$.[44] Compared with the original smooth

dx.doi.org/10.1021/am3014746 | ACS Appl. Mater. Interfaces 2012, 4, 5826–5832

copper mesh substrate, the presence of the $Cu(OH)_2$ nanostructures induces the increase of the diameter of one copper wire to about 51 μm (Figure 1e) and decreases the size of one pore to about 42 μm (Figure 1d). From the magnified image (Figure 1f), it can be readily seen that the $Cu(OH)_2$ exhibits the pine-needle-like structures with the diameter of 80−150 nm and the length of about 8 μm (see Supporting Information Figure S3). As known, such micro-/nanoscale hierarchical structures can enhance the wettability of the substrate to the extremes: superhydrophobic or superhydrophilic.[45−48]

To achieve the pH controllability, the copper mesh substrates were first coated with a layer of Au and then immersed into a mixed solution of $HS(CH_2)_9CH_3$ and $HS(CH_2)_{10}COOH$ for approximately 12 h.[21] In this way, a mixed monolayer containing both an alkyl and a carboxylic acid group can be assembled on the substrate, and the composition of the surface can be tuned by controlling the composition of the modified solution, which was confirmed by the X-ray photoelectron spectroscopy (XPS) results (see Supporting Information Figures S4 and S5). The carboxylic acid group is a special pH-responsive functional group and has been used to fabricate many pH-responsive materials, such as smart ion channel[49] and the switchable electrode.[50] Therefore, it is expected that on the copper mesh substrate modified by such monolayer the water permeation process would exhibit pH-responsivity.

The wetting properties of the films were examined by the contact angle measurements. We observed that the concentration of the $HS(CH_2)_{10}COOH$ in the modified solution has a crucial role in determining the surface wettability, and the substrate modified with X_{COOH} = 0.6 (mole fraction of $HS(CH_2)_{10}COOH$ in the modified solution) shows the best pH-responsivity (see Supporting Information Figure S6). On the flat copper substrate modified with the mixed thiol (X_{COOH} = 0.6), the contact angles for the acidic water droplet (4 μL, pH = 2) and the basic water droplet (4 μL, pH = 12) are about 93° and 66°, respectively (as a comparison, the contact angles for acidic and basic droplets on the uncoated flat copper surface have no apparent change; see Supporting Information Figure S7), while on the copper mesh films, the enhanced effect can be observed. As shown in Figure 2a, when an acidic water droplet (4 μL, pH = 2) is placed on the original smooth copper mesh film, it cannot permeate while standing on the film with a contact angle of about 106°, indicating the film is hydrophobic. As the water pH is increased, for example, pH = 12, the droplet (4 μL) spreads and permeates on the film within about 30 s, and the final contact angle is about 31°, indicating that the film becomes hydrophilic (Figure 2b).

Compared with smooth copper mesh film, the nanostructured copper film shows remarkably enhanced transition in wettability. When an acidic droplet (4 μL, pH = 2) is placed on the film, the contact angle is about 153°, indicating that the film is superhydrophobic and the droplet cannot permeate the film (Figure 2c). When a basic droplet (4 μL, pH = 12) is used, it spreads in less than 3 s, and the final contact angle is about 8°, meaning the film becomes superhydrophilic (Figure 2d). As more water is added on the film, the water can permeate and be ready to leave the film (Figure 2e−f). The superhydrophilicity (good permeability) for basic droplets and the superhydrophobicity (impermeability) for acidic droplets indicate that water permeation can be well controlled by simply adjusting the water pH.

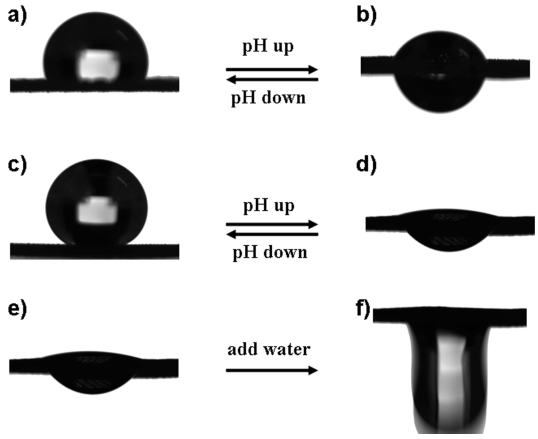

Figure 2. Water permeation for pH control on mixed thiol-modified copper mesh films (prepared with X_{COOH} = 0.6). (a, b) Photographs for an acidic droplet (4 μL, pH = 2) and a basic droplet (4 μL, pH = 12) on a smooth copper mesh film, respectively. (c) Photograph of an acidic droplet (4 μL, pH = 2) on the rough copper mesh film with a contact angle of about 153°, which means the film is superhydrophobic and the water droplet cannot permeate the film for the large negative capillary effect. (d) Basic droplet (4 μL, pH = 12) placed on the film, spreading and permeating the film when more water is added (e−f). Controllable permeation can be realized by simply controlling the water pH.

Although the smooth copper mesh film has a similar wettability transition between the hydrophobicity (106°, Figure 2a) and hydrophilicity (31°, Figure 2b), it is unsuitable for the application in the water permeation. Because the water contact angles for acidic droplets on such smooth mesh film are much lower than that on the rough mesh film, such a smooth mesh film is not sufficiently hydrophobic to prevent water leaking if small water pressure exists or under vibration. That is, a water drop cannot stand on the film stably (see Supporting Information Figure S8). Upon considering the good controllability of the water permeation, the rough copper mesh film is chosen for further study. From the above, it can be seen that the nanostructured $Cu(OH)_2$ on the substrate can not only enhance the static wettability (superhydrophobic for acidic water and superhydrophilic for basic water) but also the dynamic properties (increased antipermeation for acidic water droplets; the accelerated spreading for basic water droplets).

After being rinsed with distilled water and dried with the N_2 stream, the basic-exposed film would return to its initial superhydrophobic state for acidic droplets, indicating that the film remains pH-responsive. The reversible cycle can be repeated between the superhydrophobicity and the superhydrophilicity several times without any loss of the responsivity (Figure 3), and such responsivity does not change even over one month without special protection, indicating the film is mechanically and chemically stable.

The particular ability promises the film to be successfully utilized in practical systems. As shown in Figure 4, a rough copper mesh film with pH-responsivity was fixed to the bottom of a plastic tube. The acidic water cannot permeate the film and remains in the plastic tube (Figure 4 left, the red color for the presence of litmus). When some basic water was added to the plastic tube, the water would permeate the film and drop down to the conical flask (Figure 4 right, the blue color indicating basic water). It can be concluded that the water permeation on the film can be controlled by simply adjusting the water pH.

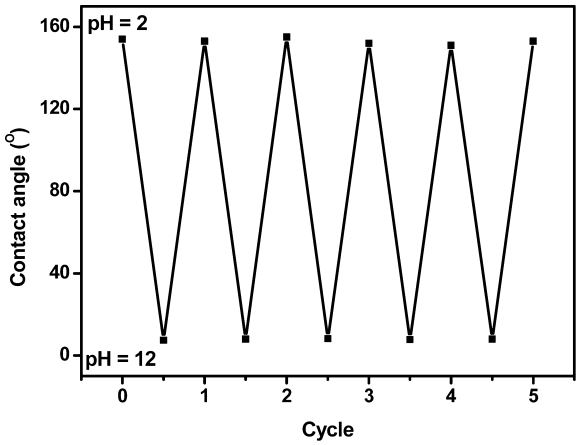

Figure 3. Reversible transition between the superhydrophobicity and superhydrophilicity on the rough copper mesh film (prepared with X_{COOH} = 0.6) can be repeated by changing the water pH alternately.

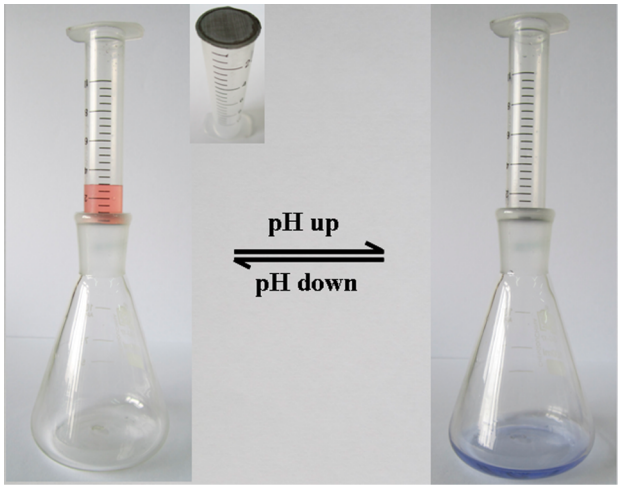

Figure 4. Schematic illustration of the pH-controllable water permeation device. The device is composed of a plastic tube with a rough structured copper mesh film fixed at one end (inset) and a conical flask as a container to collect the water. Acidic water cannot penetrate the rough mesh film (left). As the pH of the water is increased and becomes alkaline, it can penetrate the rough mesh film easily, and no water can be supported by the mesh film (right). The litmus was used as the indicator for acidic and basic water.

Furthermore, after being washed with ultrapure water and dried with a N_2 stream, the copper mesh film can restore the superhydrophobicity, and the device can be used again. Here, the device can keep the pH-controllability of the water permeation after at least ten cycles, indicating that the mesh film is stable and the device can be used repeatedly.

In addition to the reversible transition between the superhydrophobicity and the superhydrophilicity, more detailed research indicates that only the water droplet with large pH can permeate the film. From Figure 5, one can observe that the film is superhydrophobic for both acidic and neutral water. When the pH is increased from 7 to 14, the contact angles decrease dramatically, and when the pH is 12, it shows superhydrophilic property. It can be noted that in this system the water can permeate the film only when the water pH is sufficiently large (pH > 10, the film becomes hydrophilic). Similar variation can be observed on the smooth copper mesh film since the nanostructure here only takes the amplified effect.[14,15]

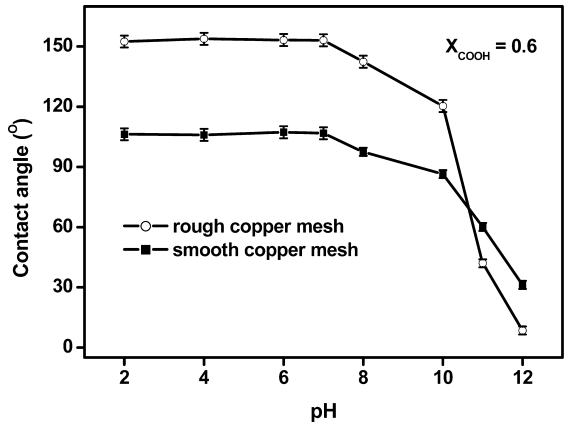

Figure 5. Contact angles as a function of water pH on smooth and rough copper mesh films prepared with X_{COOH} = 0.6, respectively.

From the above, it can be seen that the pH-responsivity of the film is crucial for the controllable water permeation, and such an ability can be ascribed to the following two reasons. The first is the protonation and deprotonation of the surface carboxylic acid groups in acidic and basic conditions, respectively.[51,52] The second is the nanostructures on the substrate which can enhance the wettability transition.[13−15] When an acidic or neutral water droplet contacts the film, the carboxylic acid groups are protonated (Figure 6a), showing relative hydrophobic property, which may be due to the lower acidity of the carboxylic acid group on the surface than that in the solution. This can be explained by the following two reasons.[51,52] The first is that the local electron constant of the carboxylic acid group is decreased in the presence of methyl groups in $HS(CH_2)_9CH_3$. The second is the hindrance effect on the formation of hydrogen bonds between the carboxylic acid and the water, resulting from the steric bulk of adjacent chains at the surface of the monolayer. Moreover, the nanostructures on the copper mesh substrate can enhance the hydrophobicity of the surface, and this can be explained as the following equation, which was proposed by Cassie and Baxter[53]

$$\cos \theta_r = f_1 \cos \theta - f_2 \quad (1)$$

Here (θ) and (θ_r) are the contact angles of the flat copper surface and the rough copper surface after modification with mixed thiol, respectively, and f_1 and f_2 are the fractions of the solid surface and air in contact with water, respectively (i.e., $f_1 + f_2 = 1$). It is easy to deduce from eq 1 that increasing f_2 increases θ_r; that is, the fraction of air in the surface is an important factor in determining the superhydrophobicity of the surface. In this work, θ = 93° (see Supporting Information Figure S7c), for smooth and nanostructured copper mesh substrates, and θ_r is 106° and 153°, respectively. According to eq 1, on the smooth and nanostructured copper mesh films, f_2 can be calculated to be 0.235 and 0.885, respectively, indicating that after introduction of nanostructured $Cu(OH)_2$ the fraction of air is increased and high enough to result in superhydrophobicity. Therefore, as shown in Figure 5, the contact angles are larger than 150° (superhydrophobic) for both acidic and neutral water. When the basic water is used, the carboxylic acid groups will be deprotonated and show hydrophilic property (Figure 6b). As the pH of the water is increased, more carboxylic acid groups on the film would be deprotonated, which can further increase the surface hydrophilic property. In this case, surface roughness can enhance the

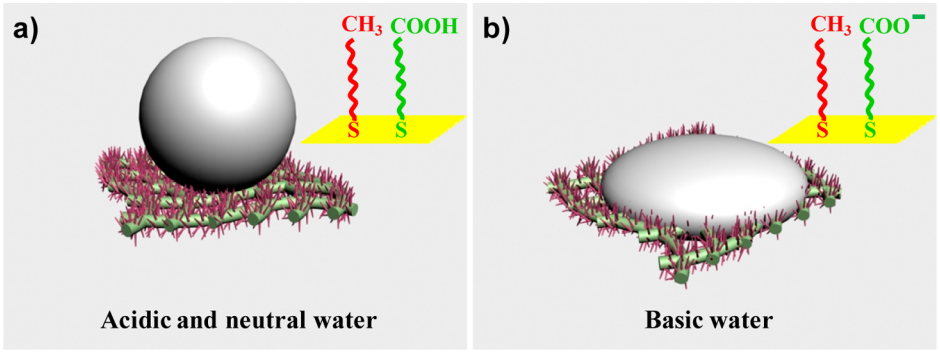

Figure 6. Schematic illustration of the shapes of the water droplets on the surfaces: (a) for acidic and neutral water, carboxylic acid groups are protonated and show hydrophobicity. Combined with the enhanced effect of the nanostructures, the film shows superhydrophobicity, and the water cannot permeate the film. (b) When basic water is used, carboxylic acid groups are deprotonated and hydrophilic; the film shows superhydrophilicity as a result of the capillary effect induced by the nanostructures; and the water can permeate the film.

hydrophilicity as described by the Wenzel equation.[54] On the copper mesh substrate, the micrometer copper wires and the nanostructured $Cu(OH)_2$ make the surface bear a large surface area and increase the surface roughness, such that the imbibition of water will occur on the rough surface as a result of the 3D capillary effect; therefore, compared with the flat copper surface modified with the same mixed thiol (the contact angle for a basic droplet is about 66°, see Supporting Information Figure S7d), the rough copper mesh film has a lower contact angle and shows superhydrophilicicity (about 8°, Figure 5).

In addition to the static properties of the wettability, the nanostructures can also greatly influence the dynamic properties of wettability.[55] For acid and neutral water, the nanostructures can help to increase the antipermeation capacity of the film (Supporting Information Figure S8). The nanostructures can not only bring a sufficient proportion of trapped air to the film, which is crucial to superhydrophobicity, but also largely improve the repellent force to water because of the size dependence of the capillary effect and the great increase in the total length of the air/water/solid triple contact line.[47] For basic water, the film becomes hydrophilic, the water filling the nanostructures first because of a much larger capillary effect than that for the usual mesh pore on the micrometer scale. Meanwhile, such nanostructures can also increase the whole spreading speed of the water droplet.[55−57] Thus, a fast wetting phenomenon and good water permeability are observed for basic water droplets. From the above, it can be concluded that both the antipermeation for acidic or neutral water and the permeability capacity for basic water can be remarkably enhanced by nanostructures.

To have a better understanding of the water permeation process, we model the process in Figure 7 on the assumption that the pores are arranged approximately in a regular square array. The position of the three-phase contact line junction, defined by α (Figure 7), is mainly governed by the differential pressure, ΔP, across the meniscus, which can be described as[58−60]

$$\Delta P = \frac{2\gamma_{LV}}{R} = \frac{2\gamma_{LV}\cos(3\pi/2 - \alpha - \theta)}{d/2 - r\sin\alpha} = -l\gamma_{LV}(\cos\theta_A)/A \quad (2)$$

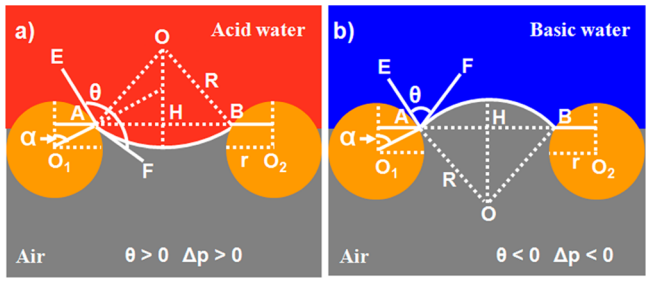

Figure 7. Schematic diagrams of the liquid wetting model of the copper mesh film. (a) For acidic water, the copper mesh film is hydrophobic ($\theta > 90°$), and water cannot permeate the film because the static pressure $\Delta P > 0$. (b) For basic water, the film is hydrophilic ($\theta < 90°$); the copper mesh film cannot withstand any pressure because the static pressure $\Delta P < 0$; and the water can permeate the film spontaneously. The position O is the center of the spherical cap that describes the meniscus; O_1 and O_2 are the cross-section center of the copper wires, $O_1O_2 = d$; A and B are the three-phase contact line positions; R is the radius of the meniscus; r is the radius of the copper wire; AE is the tangent of the circle of the cross-section of the copper wires; AF is the tangent to the meniscus.

where γ_{LV} is the surface tension of the liquid−vapor interface; R is the radius of meniscus; d is the cross-section center distance of the adjacent parallel copper wires; l is the perimeter of the pore; A is the area of the pore; θ is the intrinsic contact angle of liquid on the surface; and θ_A is the advancing contact angle of liquid on the surface. From eq 2, it is clear that the mesh film can sustain a certain pressure when $\theta > 90°$ because the static pressure $\Delta P > 0$ (negative capillary effect). Thus, the acidic and neutral water cannot permeate the film spontaneously unless external pressure is applied (Figure 7a). When the basic water is used, the surface is hydrophilic; $\theta < 90°$; $\Delta P < 0$ (capillary effect); the copper film cannot sustain any pressure; and the basic water can permeate the film spontaneously (Figure 7b). Meanwhile, from eq 2, it can also be found that ΔP increases as θ_A is increased. In this work, for acidic water, the advancing contact angles for smooth copper mesh film and rough copper mesh film are about 112° and 154°, respectively (see Supporting Information Figure S9). Thus, a larger external pressure would be needed to induce the water permeation on the rough copper mesh film than that on the smooth copper mesh film, indicating that the rough copper mesh film is more stable than the smooth copper mesh film. Calculated by eq 2, the theoretical value of the maximal pressure that the rough

copper mesh film can support is about 4.46×10^3 Pa. For the basic water, the rough copper mesh film has a lower advancing contact angle than that on the smooth copper film; thus, the water can permeate the rough copper mesh film more easily, and a good permeation effect can be achieved. Therefore, nanostructured copper mesh films can be used as controllable and stable water permeation devices.

In this work, the pore size of the copper mesh is also crucial to the film wettability, and various films (prepared with X_{COOH} = 0.6) were fabricated by using meshes with different original pore sizes. From Figure 8, it can be found that all films exhibit

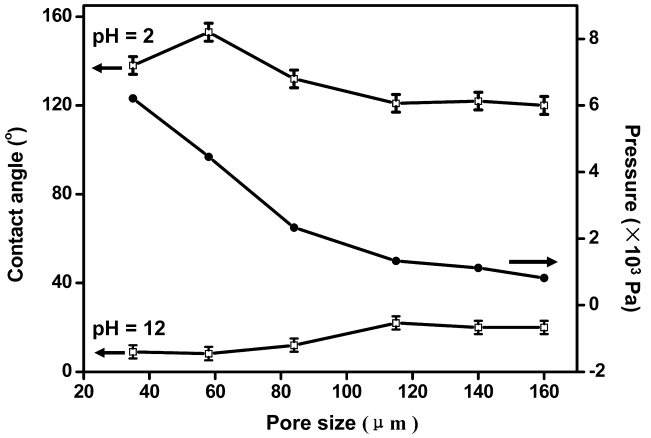

Figure 8. Dependence of the contact angles and the static pressure on the original mesh pore sizes (the film prepared by modification of the mixed thiol with X_{COOH} = 0.6 on the rough copper mesh substrate, and the static pressure for acidic water is calculated according to the eq 2). It shows that the appropriate size of the microscale mesh pores is also important in obtaining the optimum controllable performance of the film.

high hydrophilicity and good permeability for basic water, whereas the hydrophobicity for acidic water is dependent on the pore size (the pore size of the mesh film does not change after contact with acidic or basic water, see Supporting Information Figure S10). Although all films have larger contact angles compared with the flat copper surface (θ = 93°, see Supporting Information Figure S7c), only the film with pore size of about 58 μm can exhibit superhydrophobicity for acidic water droplets. When the pore size is smaller than 58 μm, although the static pressure can be increased for the decrease in the spacing between the copper wires (Figure 8, here the pressure is calculated according to eq 2, and the pressure is the maximum theoretical static pressure the mesh film can support), the fraction of liquid/solid contact (f_1 in Cassie equation) is also increased;[61] thus, according to eq 1, the contact angle would be decreased. When the pore size is larger than 58 μm, the static pressure decreases as the pore size is increased (Figure 8), which means that the hydrophobic force provided by the $Cu(OH)_2$ nanoneedles may not be enough to support the water droplet, and the water droplet would wet more copper mesh substrate and increase the fraction of liquid/solid contact f_1, which can be further confirmed by the calculated results from eq 1. For copper mesh films with pore sizes of 58, 84, 115, 140, and 160 μm, the calculated values of f_1 are 0.115, 0.349, 0.512, 0.560, and 0.593, respectively. Therefore, the films would have a lower hydrophobicity when the size of the mesh pores is increased. Because the largest difference between the wettabilities for water with different pH is favorable for good controllability, it can be inferred that ~58 μm is the optimum pore size in the original mesh film (for more detail, see Supporting Information Figure S11). Sizes above or below this value will lead to a decrease in controllability. On the basis of the above results, it can be concluded that not only the nanostructures but also the suitable size of the microscale mesh pores are important in obtaining the best controllability. The nanostructures may efficiently enhance both the permeability for basic water and the impermeability for acidic water, whereas the suitable size of the mesh pores may help to optimize the controllability.

CONCLUSIONS

In conclusion, we report a novel strategy to realize the controllable water permeation on the nanostructured copper mesh film with pH-responsive wettability. Such smart films were obtained by assembling the mixed thiol (containing both alkyl and carboxylic acid groups) on the nanostructured copper mesh substrate. For acidic or neutral water, the film shows superhydrophobic property, and the water cannot permeate the film for the presence of a large negative capillary effect resulting from the nanostructures. For basic water, the film is superhydrophilic, and the water can permeate the film easily. The water permeation process can be controlled by simply changing the water pH. The nanostructures on the substrate and the appropriate size of the microscale mesh pores can enhance not only the static wettability but also the dynamic properties. The excellent controllability of water permeation is ascribed to the combined effect of the chemical variation of the carboxylic acid group and the microstructures on the substrate. We believe that the film with such excellent controllable permeation could potentially be used in a wide range of applications, such as filtration, microfluidic device, and some separation systems.

ASSOCIATED CONTENT

Supporting Information

SEM and contact angles for samples prepared with different electrodeposition times; XPS results for samples; relationship between the contact angles and the X_{COOH}; contact angles for acidic and basic water droplets on the thiol-coated and uncoated flat copper substrates; advancing and receding contact angles; contrast results of the antipermeation between the hydrophobic and the superhydrophobic copper mesh film. This material is available free of charge via the Internet at http://pubs.acs.org.

AUTHOR INFORMATION

Corresponding Author

*E-mail: keningsunhit@163.com. Tel.: (+86) 045186412153. Fax: (+86) 045186412153.

Author Contributions

All authors have given approval to the final version of the manuscript. Zhongjun Cheng and Ming Du contributed equally.

Notes

The authors declare no competing financial interest.

ACKNOWLEDGMENTS

This work is supported by the Open Project of State Key Laboratory of Urban Water Resource and Environment, Harbin Institute of Technology (No. ES201007); Project (HIT.

NSRIF. 2009079) Supported by Natural Scientific Research Innovation Foundation in Harbin Institute of Technology; China Postdoctoral Science Foundation funded project (20100471045) and (201104428); The Research Fund for the Doctoral Program of Higher Education (20112302120062).

REFERENCES

(1) Murata, K.; Mitsuoka, K.; Hirai, T.; Walz, T.; Agre, P.; Heymann, J. B.; Engel, A.; Fujiyoshi, Y. *Nature* **2000**, *407*, 599−605.
(2) de Groot, B. L.; Grubmuller, H. *Science* **2001**, *294*, 2353−2357.
(3) Corry, B. *J. Phys. Chem. B* **2008**, *112*, 1427−1434.
(4) Chen, W.; Su, Y.; Peng, J.; Zhao, X.; Jiang, Z.; Dong, Y.; Zhang, Y.; Liang, Y.; Liu, J. *Environ. Sci. Technol.* **2011**, *45*, 6545−6552.
(5) Allen, R.; Melchionna, S.; Hansen, J. P. *Phys. Rev. Lett.* **2002**, *89*, 175502−175505.
(6) Zhu, F. Q.; Tajkhorshid, E.; Schulten, K. *Phys. Rev. Lett.* **2004**, *93*, 224501−224504.
(7) Yu, M.; Noble, R. D.; Falconer, J. L. *Acc. Chem. Res.* **2011**, *44*, 1196−1206.
(8) Wan, R.; Li, J.; Lu, H.; Fang, H. *J. Am. Chem. Soc.* **2005**, *127*, 7166−7170.
(9) Williams, M. E.; Stevenson, K. J.; Massari, A. M.; Hupp, J. T. *Anal. Chem.* **2000**, *72*, 3122−3128.
(10) Su, J.; Guo, H. *ACS Nano* **2011**, *5*, 351−359.
(11) Ariga, K.; Okahata, Y. *J. Am. Chem. Soc.* **1989**, *111*, 5618−5622.
(12) Niwa, M.; Mukai, A.; Higashi, N. *Langmuir* **1990**, *6*, 1432−1434.
(13) Xin, B.; Hao, J. *Chem. Soc. Rev.* **2010**, *39*, 769−782.
(14) Liu, K.; Yao, X.; Jiang, L. *Chem. Soc. Rev.* **2010**, *39*, 3240−3255.
(15) Li, X. M.; Reinhoudt, D.; Crego-Calama, M. *Chem. Soc. Rev.* **2007**, *36*, 1350−1368.
(16) Sun, T.; Wang, G.; Feng, L.; Liu, B.; Ma, Y.; Jiang, L.; Zhu, D. *Angew. Chem., Int. Ed.* **2004**, *43*, 357−360.
(17) Feng, X.; Feng, L.; Jin, M.; Zhai, J.; Jiang, L.; Zhu, D. *J. Am. Chem. Soc.* **2004**, *126*, 62−63.
(18) Feng, X.; Zhai, J.; Jiang, L. *Angew. Chem., Int. Ed.* **2005**, *44*, 5115−5118.
(19) Xu, L.; Chen, W.; Mulchandani, A.; Yan, Y. *Angew. Chem., Int. Ed.* **2005**, *44*, 6009−6012.
(20) Minko, S.; Muller, M.; Motornov, M.; Nitschke, M.; Grundke, K.; Stamm, M. *J. Am. Chem. Soc.* **2003**, *125*, 3896−3900.
(21) Yu, X.; Wang, Z. Q.; Jiang, Y. G.; Shi, F.; Zhang, X. *Adv. Mater.* **2005**, *17*, 1289−1293.
(22) Xia, F.; Ge, H.; Hou, Y.; Sun, T.; Chen, L.; Zhang, G.; Jiang, L. *Adv. Mater.* **2007**, *19*, 2520−2524.
(23) Prins, M. W. J.; Welters, W. J. J.; Weekamp, J. W. *Science* **2001**, *291*, 277−280.
(24) Krupenkin, T. N.; Taylor, J. A.; Schneider, T. M.; Yang, S. *Langmuir* **2004**, *20*, 3824−3827.
(25) Zhu, L.; Xu, J.; Xiu, Y.; Sun, Y.; Hess, D. W.; Wong, C. P. *J. Phys. Chem. B* **2006**, *110*, 15945−15950.
(26) Wang, Z. K.; Ci, L. J.; Chen, L.; Nayak, S.; Ajayan, P. M.; Koratkar, N. *Nano Lett.* **2007**, *7*, 697−702.
(27) Verplanck, N.; Galopin, E.; Camart, J. C.; Thomy, V.; Coffinier, Y.; Boukherrou, R. *Nano Lett.* **2007**, *7*, 813−817.
(28) McHale, G.; Herbertson, D. L.; Elliott, S. J.; Shirtcliffe, N. J.; Newton, M. I. *Langmuir* **2007**, *23*, 918−924.
(29) Wang, R.; Hashimoto, K.; Fujishima, A.; Chikuni, M.; Kojima, E.; Kitamura, A.; Shimohigoshi, M.; Watanabe, T. *Nature* **1997**, *388*, 431−432.
(30) Lim, H. S.; Han, J. T.; Kwak, D.; Jin, M. H.; Cho, K. *J. Am. Chem. Soc.* **2006**, *128*, 14458−1459.
(31) Zhang, X. T.; Sato, O.; Fujishima, A. *Langmuir* **2004**, *20*, 6065−6067.
(32) Wang, S.; Feng, X.; Yao, J.; Jiang, L. *Angew. Chem., Int. Ed.* **2006**, *45*, 1264−1267.
(33) Lim, H. S.; Kwak, D.; Lee, D. Y.; Lee, S. G.; Cho, K. *J. Am. Chem. Soc.* **2007**, *129*, 4128−4129.
(34) Zhu, W.; Feng, X.; Feng, L.; Jiang, L. *Chem. Commun.* **2006**, 2753−2755.
(35) Yan, B.; Tao, J.; Pang, C.; Zheng, Z.; Shen, Z.; Huan, C.; Yu, T. *Langmuir* **2008**, *24*, 10569−10571.
(36) Kwon, Y.; Weon, B. M.; Won, K. H.; Je, J. H.; Hwu, Y.; Margaritono, G. *Langmuir* **2009**, *25*, 1927−1929.
(37) Cooper, C. G. F.; MacDonald, J. C.; Soto, E.; McGimpsey, W. G. *J. Am. Chem. Soc.* **2004**, *126*, 1032−1033.
(38) Jones, D. M.; Smith, J. R.; Huck, W. T. S.; Alexander, C. *Adv. Mater.* **2002**, *14*, 1130−1134.
(39) Halldorsson, J. A.; Little, S. J.; Diamond, D.; Spinks, G.; Wallace, G. *Langmuir* **2009**, *25*, 11137−11141.
(40) Song, W.; Xia, F.; Bai, Y.; Liu, F.; Sun, T.; Jiang, L. *Langmuir* **2007**, *23*, 327−331.
(41) Tian, D.; Zhang, X.; Zhai, J.; Jiang, L. *Langmuir* **2011**, *27*, 4265−4270.
(42) Xue, Z.; Wang, S.; Lin, L.; Chen, L.; Liu, M.; Feng, L.; Jiang, L. *Adv. Mater.* **2011**, *23*, 4270−4273.
(43) Zhang, L.; Zhang, Z.; Wang, P. *NPG Asia Mater.* **2012**, e8.
(44) Wu, X.; Bai, H.; Zhang, J.; Chen, F.; Shi, G. *J. Phys. Chem. B* **2005**, *109*, 22836−22842.
(45) Lafuma, A.; Quéré, D. *Nat. Mater.* **2003**, *2*, 457−460.
(46) Roach, P.; Shirtcliffe, N. J.; Newton, M. I. *Soft Matter* **2008**, *4*, 224−240.
(47) Gao, X.; Jiang, L. *Nature* **2004**, *432*, 36−36.
(48) Xiu, Y.; Zhu, L.; Hess, D. W.; Wong, C. P. *Nano Lett.* **2007**, *7*, 3388−3393.
(49) Hou, X.; Liu, Y.; Dong, H.; Yang, F.; Li, L.; Jiang, L. *Adv. Mater.* **2010**, *22*, 2440−2443.
(50) Liu, D.; Liu, H.; Hu, N. *Electrochim. Acta* **2010**, *55*, 6426−6432.
(51) Holmes-Farley, S. R.; Bain, C. D.; Whitesides, G. M. *Langmuir* **1988**, *4*, 921−937.
(52) Bain, C. D.; Whitesides, G. M. *Langmuir* **1989**, *5*, 1370−1378.
(53) Cassie, A. B. D.; Baxter, S. *Trans. Faraday Soc.* **1944**, *40*, 546−551.
(54) Wenzel, R. N. *Ind. Eng. Chem.* **1936**, *28*, 988−994.
(55) Chaudhury, M. K.; Whitesides, G. M. *Science* **1992**, *256*, 1539−1541.
(56) Karkare, M. V.; Fort, T. *Langmuir* **1993**, *9*, 2398−2403.
(57) Starov, V. M.; Zhdanov, S. A.; Kosvintsev, S. R.; Sobolev, V. D.; Velarde, M. G. *Adv. Colloid Interface Sci.* **2003**, *104*, 123−158.
(58) Youngblood, J. P.; McCarthy, T. J. *Macromolecules* **1999**, *32*, 6800−6806.
(59) Liu, B.; Lange, F. F. J. *Colloid Interface Sci.* **2006**, *298*, 899−909.
(60) Tian, D.; Zhang, X.; Wang, X.; Zhai, J.; Jiang, L. *Phys. Chem. Chem. Phys.* **2011**, *13*, 14606−14610.
(61) Zheng, Q. -S.; Yu, Y.; Zhao, Z. -H. *Langmuir* **2005**, *21*, 12207−12212.